Frequency Extrapolation for Carrier Aggregation as a Super-Resolution Problem: Rethinking Conventional Forecasting Methods

Daoud Burghal
Standard and Mobility (SMI) Team
Samsung Research America,
Mountain View, CA, USA
d.burghal@samsung.com

Yan Xin
Standard and Mobility (SMI) Team
Samsung Research America,
Berkeley Heights, NJ, USA
yan.xin@samsung.com

Jianzhong (Charlie) Zhang
Standard and Mobility (SMI) Team
Samsung Research America,
Plano, TX, USA
jianzhong.z@samsung.com

Abstract

Frequency extrapolation plays a pivotal role in modern wireless communication systems, particularly in Carrier Aggregation (CA), where service providers combine multiple Carrier Components (CCs) to enhance system throughput (Tput). This technique enables the efficient utilization of available spectrum, ensuring robust and high-performance connectivity. However, the effectiveness of CA heavily relies on accurate Channel State Information (CSI) for each CC, which is essential for tasks such as precoding and User Equipment (UE) coordination. In practice, obtaining CSI beyond the primary CC (Primary Cell, PCell) is challenging, necessitating advanced prediction methods to estimate CSI for secondary CCs (SCell).

Frequency extrapolation can be framed as a series forecasting problem, where the goal is to predict future CSI values based on historical data. Traditional time-series forecasting methods, while effective in many domains, fall short in the context of wireless communication. This is due to the unique challenges posed by the dynamic and multi-user nature of wireless environments, where predictions must account for varying signal characteristics across multiple users and scenarios. To address these limitations, this work redefines frequency extrapolation as a super-resolution (SR) problem, leveraging advanced deep learning techniques to enhance the accuracy and robustness of CSI predictions.

In this study, we propose a novel solution that applies SR to combined CCs in the inverse domain (delay domain). By utilizing state-of-the-art deep learning algorithms, including vision-based transformers, we demonstrate that our approach outperforms existing AI-based solutions. Our simulation results highlight the superior prediction robustness and significant throughput gains achieved over a wide frequency range, reaffirming the potential of SR techniques in revolutionizing frequency extrapolation for CA.

39th Conference on Neural Information Processing Systems (NeurIPS 2025) Workshop: AI and ML for Next-Generation Wireless Communications and Networking (AI4NextG).

1 Introduction

Carrier Aggregation (CA) is one of the key features in modern cellular communication systems. It is usually used to boost the system Tput, where the service provider can aggregate more than one Component Carrier (CC) to extend the used spectrum for one or more User Equipment (UE). To fully utilize the available spectrum, CSI is needed for many tasks, including precoding for Massive multiple-input multiple-output (MIMO). Currently, the network can acquire the CSI with Sounding Reference Signal (SRS) or PMI type II in the primary CC (also known as Primary Cell (PCell)), while the other CCs have limited CSI information, e.g., through PMI type I, resulting in performance degradation, especially for multi-user MIMO system. To address this issue, CSI prediction can be used to extrapolate the CSI into the secondary CCs (SCells).

Recently, Machine Learning (ML) was proposed in the literature to solve the CSI extrapolation. Typically, an AI solution relies on AI model that learns the mapping between the observed PCell CSI and the SCell's CSI. However, it has been noticed that the solutions struggle in certain environments, e.g., dense Non-Line of Sight (NLOS), or when the environment is sparsely sampled (large distances between data points) [7, 1]. Unfortunately, in practice, both conditions are present.[1] To address these issues, we proposed a novel AI solution that utilizes (i) the fact that transforming *combined* CCs into *delay* provides a high-resolution "image" of the PCell only, (ii) advanced Computer Vision (CV) architectures for SR and image restoration, such as Shifted Window (Swin) transformer, and (iii) UE pre-selection. For UE pre-selection, we develop a lightweight AI solution that can predict whether the CSI prediction for a given UE is possible or whether a simple commercially available solution (e.g., PMI) is enough. This is important since the available dataset still impacts the quality of the AI-based CSI prediction.

1.1 Related Work

Frequency extrapolation has been extensively studied in the wireless communication literature, encompassing both classical signal processing solutions and AI-based approaches. Classical methods, however, face significant challenges due to the high nonlinearity of the problem, computational complexity, and sensitivity to modeling limitations and noise [8]. In recent years, deep learning solutions have garnered considerable attention. Nevertheless, recent studies highlight the complexity of the problem: for instance, CNN and MLP-based architectures often struggle to train effectively in complex environments [1], while other works emphasize the need for very high sample densities to achieve accurate extrapolation [7]. In this paper, we propose a novel approach that leverages advances in computer vision and fundamental signal processing concepts. We frame the problem as a super-resolution task in the delay domain, where the observed CC provides a low-resolution image. The super-resolution (SR) network then learns to recover plausible high-resolution details based on the ensemble of signals in the dataset.

This problem can be viewed as a combination of denoising and forecasting. With the advent of transformers, series forecasting has gained significant attention in the AI community. For example, Informer [13] introduced efficient ProbSparse attention for long sequences, while FEDformer [14] enhanced seasonal-trend decomposition with Fourier-based attention. However, critical studies have shown that the conventional formulation of series forecasting (SF) with transformers can be challenged. iTransformer [4] revisits the input orientation by inverting the signal, while other works suggest that simple linear neural networks (NNs) can potentially perform well [11]. Recently, FITS proposed using interpolation in the inverse domain (frequency domain) for SF [10]. While these contributions are significant, series forecasting in the wireless domain presents unique challenges. These include multi-asset prediction, where each series may belong to a different user (UE) or environment. Additionally, CSI prediction involves complex signals, making joint prediction of real and imaginary components (due to phase rotation) essential, which calls for specialized multivariate prediction techniques.

[1] This is true, at least for the near-term system deployment, where, e.g., only a subset of UEs are capable of sending reference signals at multiple CCs, resulting in a small dataset and/or sparsely sampled environments.

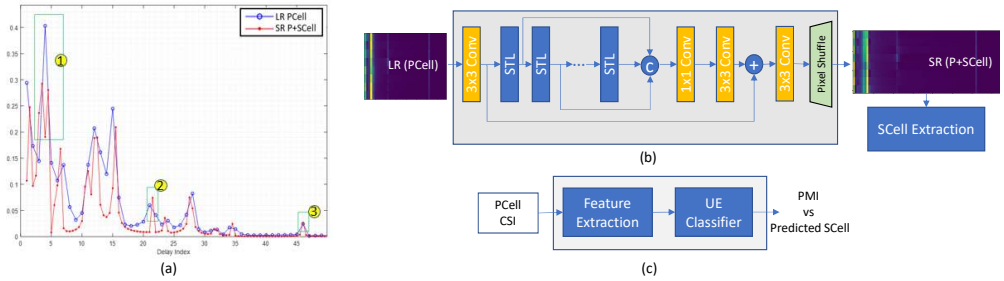

Figure 1: Illustration of the SR concept with solution. (a) An example of a PCell vs joint PCell and SCell in delay domain. Notice several scenarios could show up when including higher frequencies, certain peaks could (1) shrink, (2) get shifted, or (3) preserved. (b) A proposed network architecture, STL stands for Swin transformer layer. (c) UE pre-selection to decide whether the SCell prediction is useful, e.g., for pre-coding.

1.2 Paper Structure and Main Results

In Section 2, we cover the system model and problem statement. Section 3 discusses Carrier Aggregation as a Super-resolution problem, including its formulation. Section 4 presents our proposed solution. Section 5 evaluates the prediction accuracy and achieved throughput. In the appendix A, explores performance enhancement through user preselection. Finally, Section B compares our method with conventional series forecasting.

In this paper we carry out simulation studies over a relatively large bandwidth. The results show that the proposed transformation provides more than 5 dB NMSE gain to state-of-the-art AI solutions (100% gain). We also use link-level simulation to evaluate the rank-2 Tput against the existing commercial solution (PMI-type1) and other upper bounds. The proposed solution beats the PMI-type1 and approaches the upper bound, especially with UE pre-selection. Furthermore, in the appendix we show sample result that indicate that our proposed solution can be competitive approach for typical Time-Series Forecasting, while other approaches might struggle in CA problem.

2 System Model and Problem Statement

We consider a single-cell wireless system where a BS is equipped with a dual-polarized uniform planar array (UPA) with $N_h \times N_v$ antennas in the horizontal and the vertical domain, respectively. The BS communicates with a UE that is equipped with N_u antenna elements. We assume a CA system consists of a PCell and an SCell that use Orthogonal Frequency Division Multiplexing (OFDM) with K^p and K^s Resource Blocks (RBs), in the PCell and SCell, respectively. Let $\mathbb{G}^{(p)} \in \mathcal{C}^{2\times N_h \times N_v \times K^p \times N_u}$ be the observed signal in PCell, acquired through SRS. The $\mathbb{G}^p$ is used to predict the CSI in SCell, $\mathbb{G}^{(s)}$, i.e.,

$$\widehat{\mathbb{G}}^{(s)} = \mathcal{P}_{\mathbf{\Theta}} \left(\mathbb{G}^{(p)} \right), \tag{1}$$

where $\mathcal{P}_{\mathbf{\Theta}}$ is the channel prediction function parameterized by $\mathbf{\Theta}$. The $\widehat{\mathbb{G}}^{(s)}$ can then be used to derive the downlink precoders and possibly assist in other tasks. The goal is to learn a mapping function $\mathcal{P}_{\Theta}$ such that it resembles closely the true mapping $\mathcal{P}$.

3 CA as a Super-resolution Problem

In CV domain, the Super-resolution refers to the process that aim to recover the High-Resolution (HR) image $\mathbb{R}$ from a Low-Resolution (LR) image $\mathbb{L}$. Typically, the LR image is assumed to be HR images that has gone through one or more degradation processes $\mathcal{D}$ [9], such as blurring and sub-sampling.

$$\mathbb{L} = \mathcal{D}(\mathbb{R})$$

The blurring process can sometimes be represented by a filtering process, such as a linear smoothing low pass filter. In such a case, the filters can be convolved with the HR image to produce the LR image. The shape of the filter depends on the type of the kernel w. In the frequency domain, the linear filtering process can be represented by the multiplication of the filter W with the image.

$$\mathbb{L} = w * \mathbb{R} \overset{\text{Time (Space)/Frequency}}{\longleftrightarrow} W\mathcal{F}\{\mathbb{R}\},$$

where $\mathcal{F}\{\}$ is the Fourier Transform and '$*$' is convolution operation. An ideal low-pass filter can be used to remove high-frequency components that typically include high-frequency noise, as well as sharp edges, and contrasts in images. Thus, recovering the high-frequency components can increase the resolution of the image.

For CA, we can view observing PCell (i.e., receiving the PCell CSI only) as filtering out the SCell CSI, i.e., we have:

$$\mathbb{G}^{(p)} = W[\mathbb{G}^{(p)}, \mathbb{G}^{(s)}].$$

However, unlike CV images, sharp edges have different interpretations in wireless systems. Increasing the bandwidth impacts whether propagation paths can be resolved in the delay domain. To elaborate, the received signal is a result of the superposition of multi-path components (MPCs); each MPC represents interactions between the transmitted signal and one or more scatters in the environment. Each MPC may have a different delay value. System bandwidth is inversely proportional to the width of the delay bins and whether an MPC can be resolved [6]. Thus, delay domain representation of the extended (here with CA) results in a higher delay resolution of the channel. Fig. 1-(a) shows an illustrative example.

4 Proposed Solution

4.1 SR Solution

Let $\widehat{\mathbb{H}}^{(p)}$, $\widehat{\mathbb{H}}^{(s)}$ and $\widehat{\mathbb{H}}^{(ps)}$, represent the PCell, SCell and joint PCell SCell channel in delay domain. The $\widehat{\mathbb{H}}^{(ps)}$ is transformed after spectrum extension, i.e.,

$$\mathbb{H}^{(ps)} = \mathcal{F}^{-1}[\mathbb{G}^{(p)}, \mathbb{G}^{(s)}].$$

Then in the proposed solution, we have

$$\widehat{\mathbb{H}}^{(ps)} = \mathcal{P}_{\mathbf{\Theta}}\left(\mathbb{H}^{(p)}\right).$$

Once $\widehat{\mathbb{H}}^{(ps)}$ is obtained, the a Fourier transform followed by SCell extraction is performed. To learn $\mathcal{P}_{\mathbf{\Theta}}$, we utilize a SR Neural Network architectures from the CV domain.

Although in this work we focus on a setup where the PCell and SCell are adjacent to one another and that SCell CCs at higher frequency, other options are also possible in the standards. The SR discussion above is still valid, but the recovery process can sometimes be referred to as image restoration.

4.2 The AI model for Super Resolution

We consider vision transformer-based SR solution, in particular, the Shifted Window (Swin) vision transformer [5]. The Swin architecture has proved to be successful over many different CV tasks, retaining the benefits of the attention mechanism while avoiding the high computational complexity of the vanilla transformers.

In this paper, the proposed solution is inspired by earlier work, such as the SwinIR [3] and [2]. As depicted in 1 (b), the proposed deep learning model consists of the following components. A CNN layer that represents a learnable encoding layer (also called shallow feature extraction). This layer maps the real/imaginary of the original complex-valued channel image into a larger feature space (e.g., 20 features in this paper), aiming to facilitate the subsequent processing. The main body of the proposed model follows the first CNN layer, where it contains six sequential Swin Transformer Layers (STLs). Each STL is further comprised of two window attention based transformer layers: The first layer performs normal window attention on the 3D feature maps while the second performs shifted window attention with an objective of increasing the reception field of the model to mitigate the sub-optimality of window partitioning. The output of each STL is sequentially fed to the following STL. Moreover, to increase the model capacity, these learned intermediate features are also being concatenated along with the output of all previous STLs. These concatenated features are then combined with 1D CNN layer and an adaptation CNN layer. A long residual skip connection is also adopted to enhance the learning stability of the solution. Finally, the dimension reduction and tuning

Table 1: Hyper-parameters for model training

Parameter	Value
B (Batch size)	64
Number of epochs	150
Initial learning rate	1×10^{-3}
Learning rate schedule	$0.1@[70, 110, 140]$
Train/Validation/Testing	85%/ 5%/ 10%
Loss function	NMSE

are performed with a CNN layer that employs 3×3 kernels. As highlighted in [2], the model is lightweight, thanks to the CNN layers, requiring a small number of trainable parameters.

The input to the model is a preprocessed $\mathbb{H}^{(p)}$ signal, where the PCell CSI is normalized so that it has unit power. The signal is also reshaped as a 2D image $2 \times 2N_h N_v \times K^p$, where the first dimension represents the number of channels (the real and imaginary parts). The different UE antennas are processed separately. At the output, the normalized HR channel (combination of PCell and SCell) is predicted, with output shape $2 \times 2N_h N_v \times (K^p + K^s)$. The signal is then processed to extract the SCell CSI.

5 Evaluation

We use link level simulation to acquire dataset to train and test the proposed solution.

5.1 Metrics and Benchmarks

For fair comparison against several baselines, we use two metrics.

- The Normalized Mean Square Error (NMSE): used to assess the quality of SCell prediction, and compare to other AI solutions.
- Tput: The achieved down-link data rate in SCell. The SCell prediction is used to design precoder that can be used for downlink communication. In this paper, we focus on SU-MIMO evaluations. We use this metric to compare the performance against the commercial baselines.

The considered baselines are two categories:

- AI baselines for SCell prediction. We have implemented to several popular and recent AI solutions. We here focus on two of them, the work in [1],"Arnold", is one of the early works for frequency extrapolation, the proposed model is based on Fully Connected Neural Network. The other is [12], "CV-3DCNN", which uses complex valued NN with CNN architecture for frequency extrapolation.
- Tput baselines. We use PMI-type1 as the first baseline since it is a widely used solution in SCell. We further consider genie-based precoding at RB level and at sub-band levels, with sub-band size = 4. The genie can be viewed as an upper bound on the achieved Tput.

5.2 Dataset

The dataset considers a MIMO-OFDM system where the base station employs a 4×4 dual-polarized UPA. The wireless channel follows the 3GPP Urban Micro (UMi) channel model with a central frequency of 3.6 GHz and channel bandwidth 100 MHz for both PCell and SCell, i.e., a total of 200 MHz when CA is used, and each CC uses 272 RBs ($K^{(p)} = K^{(s)} = 272$). The UEs are collected from three different sites, each has roughly 660 UEs. 10% of the used are reserved for testing. Each UE has two antennas and is moving at 3 kmph. The PCell SRS periodicity is assumed to be 10 ms. For each UE we collect SRS over 0.1 s. Finally, we assume the system is operating at 20 dB SNR.

Finally, the training information is shown in the table1.

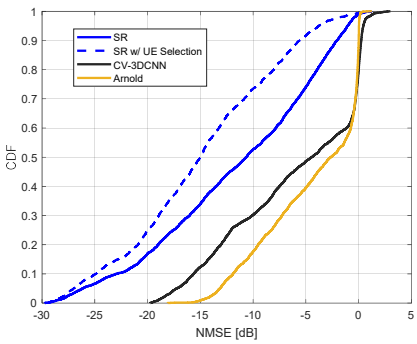

Figure 2: The CDF of NMSE in dB for the predicted CSI.

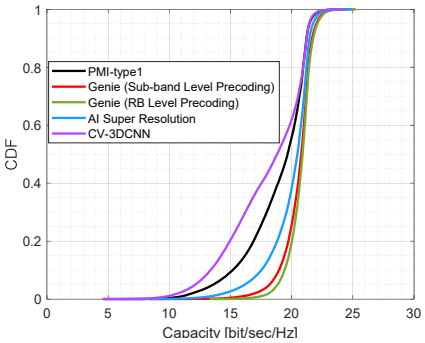

Figure 3: The CDF of achieved rank-2 Tput.

5.3 Results

5.3.1 Prediction Accuracy

The channel prediction accuracy is typically used in the literature to illustrate the performance of frequency extrapolation. Metrics such as NMSE and MSE are also used as cost functions during the model training. Thus, it is an important metric for comparative study. Fig. 2 shows the NMSE results against the two AI solutions. The advantage of the proposed solution is evident. 5 dB gain is observed at the 50th percentile. As we will discuss below, we observed a sub-optimal performance of the plotted benchmarks. This has also been reported in earlier works, even in [1], where it was observed that conventional AI solution struggles in certain environments with low data density, a typical scenario for the SCell prediction problem.

Note that even with the proposed solution (and using the above dataset), 10% of the UEs have a high NMSE. This can be partially attributed to the dataset (as discussed in A). To address this issue, we apply the UE pre-selection. For the subset of selected UEs, the median NMSE is reduced by 5 dB, along with less than 3% of UEs that have high NMSE.

5.3.2 Achieved Tput

Next, we assume that the two UE antennas are used for rank-2 communication. Fig. 3 shows the Tput for different solutions. We first notice that the proposed AI solution outperforms the commercial baseline and the AI (CV-3DCNN) baseline (the other baseline is omitted for clarity). It is also close to the genie solutions that assume more knowledge about the SCell channel state.

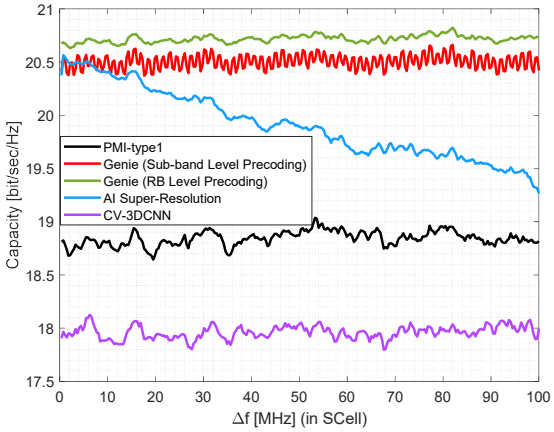

Figure 4: Tput over SCell RBs, Δf represents the frequency distance from the closest PCell RB.

Since the proposed solution predicts the channel state at every RB, it is interesting to show the performance over every RB. To demonstrate that, in Fig. 4, we plot the calculated Tput for the different solutions. We notice that while the solution shows good predictive ability at RBs close to the

observed PCell RBs, it still deteriorates due to the complexity of the channel prediction. Furthermore, we notice that the other AI solution struggles at all RB, which raises the question of its learning ability in this diverse dataset.

6 Conclusions

In this paper, we considered the CSI acquisition in the CA problem. We propose an AI solution for SCell channel prediction. The proposed solution utilizes a novel formulation of the CA as SR. We propose a vision transformer-based architecture based on the Swin transformer to solve the SR problem. We further address the problem of data limitation in CA problem through UE pre-selection that can determine whether the CSI prediction is feasible. The simulation studies show that the proposed solution outperforms baselines in NMSE and Tput and approaches the ideal Tput with UE pre-selection.

Acknowledgments

The authors would like to thank Yu Zhang, Yong Ren, Hao Chen, Shawn Ma, Bassel Abou Ali Modad, Yeqing Hu, and Yang Li for their insightful discussions and valuable assistance.

References

[1] Maximilian Arnold et al. Enabling fdd massive mimo through deep learning-based channel prediction. *arXiv preprint arXiv:1901.03664*, 2019.

[2] Jinsheng Fang et al. A hybrid network of cnn and transformer for lightweight image super-resolution. In *Proc. of the IEEE/CVF conf. on computer vision and pattern recog.*, pages 1103–1112, 2022.

[3] Jingyun Liang, Jiezhang Cao, Guolei Sun, Kai Zhang, Luc Van Gool, and Radu Timofte. Swinir: Image restoration using swin transformer. In *Proceedings of the IEEE/CVF international conference on computer vision*, pages 1833–1844, 2021.

[4] Yong Liu, Tengge Hu, Haoran Zhang, Haixu Wu, Shiyu Wang, Lintao Ma, and Mingsheng Long. itransformer: Inverted transformers are effective for time series forecasting. *arXiv preprint arXiv:2310.06625*, 2023.

[5] Ze Liu, Yutong Lin, Yue Cao, Han Hu, Yixuan Wei, Zheng Zhang, Stephen Lin, and Baining Guo. Swin transformer: Hierarchical vision transformer using shifted windows. In *Proceedings of the IEEE/CVF international conference on computer vision*, pages 10012–10022, 2021.

[6] Andreas F Molisch. *Wireless communications: from fundamentals to beyond 5G*. John Wiley & Sons, 2022.

[7] Michael Neuman, Daoud Burghal, and Andreas F Molisch. Impact of channel and system parameters on performance evaluation of frequency extrapolation using machine learning. *IEEE Open Journal of the Communications Society*, 2025.

[8] François Rottenberg, Rui Wang, Jianzhong Zhang, and Andreas F Molisch. Channel extrapolation in fdd massive mimo: Theoretical analysis and numerical validation. In *2019 IEEE Global Communications Conference (GLOBECOM)*, pages 1–7. IEEE, 2019.

[9] Zhihao Wang, Jian Chen, and Steven CH Hoi. Deep learning for image super-resolution: A survey. *IEEE transactions on pattern analysis and machine intelligence*, 43(10):3365–3387, 2020.

[10] Zhijian Xu, Ailing Zeng, and Qiang Xu. Fits: Modeling time series with $10k$ parameters. *arXiv preprint arXiv:2307.03756*, 2023.

[11] Ailing Zeng, Muxi Chen, Lei Zhang, and Qiang Xu. Are transformers effective for time series forecasting? In *Proceedings of the AAAI conference on artificial intelligence*, volume 37, pages 11121–11128, 2023.

[12] Yibin Zhang et al. Cv-3dcnn: Complex-valued deep learning for csi prediction in fdd massive mimo systems. *IEEE Wireless Comm. Lett.*, 10(2):266–270, 2020.

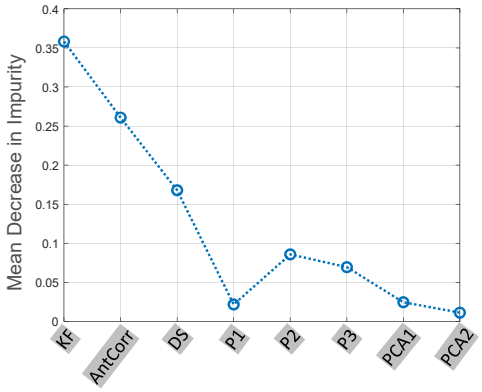

Figure 5: The MDI of different features, the higher MDI level can indicate higher impact.

[13] Haoyi Zhou, Shanghang Zhang, Jieqi Peng, Shuai Zhang, Jianxin Li, Hui Xiong, and Wancai Zhang. Informer: Beyond efficient transformer for long sequence time-series forecasting. In *Proceedings of the AAAI conference on artificial intelligence*, volume 35, pages 11106–11115, 2021.

[14] Tian Zhou, Ziqing Ma, Qingsong Wen, Xue Wang, Liang Sun, and Rong Jin. Fedformer: Frequency enhanced decomposed transformer for long-term series forecasting. In *International conference on machine learning*, pages 27268–27286. PMLR, 2022.

A User Pre-Selection

As discussed earlier, it is expected that the number of data points that have PCell-SCell pairs to be limited (in number and/or spatial density) due to the challenge of collecting the CSI in the SCell. That can be attributed to UE capabilities, network configuration, and system stability. However, we have observed that the diversity of the data points in the dataset impacts the quality of the SCell prediction. Furthermore, we observed that the challenging data points for SCell prediction might not be well represented in the training dataset. In this subsection, we propose a few channel properties (features) that can be used to measure the similarity between data points. We also design a simple ML, e.g., random-forest, solution to infer whether a data point (during system operation) can be reliably predicted. Fig. 1-(c), illustrate the flow.

In order to extract simple features, we studied a few condensed wireless channel parameters along with a number of statistical features [6]. The set of features includes (i) the delay spread "DS", (ii) the antenna correlation "AntCorr", (iii) K-factor "KF", (iv) Mean power "P1", (v) maximum power "P2", and (vi-vii) the first and second principal components from PCA dimensionality reduction solution "PCA1" and "PCA2". The impact of the features is studied against the Mean Decrease Impurity (MDI) in a Random Forest classifier. The classification is based on the performance of AI solution on the *training* dataset. To overcome the limitation of the MDI of RF, we used several data splits and random seeds to train the RF and average the MDI. The MDI values for some of the features are shown in Fig. 5. As the figure suggests, DS, AntCorr, and KF serve as good feature candidates for predicting the SCell prediction performance. This is expected, as all three values can indicate LOS vs NLOS and the severity of scattering in the environment. To judge whether two data points are similar, we use the Radial basis function kernel, given by:

$$d(p_i, p_j) = e^{\frac{||\boldsymbol{x}_i - \boldsymbol{x}_j||^2}{2\sigma}},$$

where $\boldsymbol{x}_i \in \mathcal{R}^3$ contains the normalized values of the three features for points i, and σ is design parameter. During the online operation, we extract the feature from the observed PCell of the given UE, calculate the feature distance $d(.,.)$ to the stored points in the dataset, and use that, along with the accuracy of these points, as an input feature to the random forest model to classify whether the UE should rely on AI-based SCell prediction or other solution (e.g., PMI).

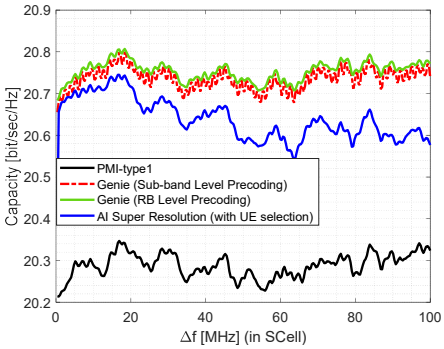

Figure 6: Tput calculated at every SCell RBs. The UE are pre-selected based on UE classification solution, Δf represent the frequency distance from the closest PCell RB.

Table 2: Multi-variate forecasting performance comparison (lower is better). Input and output are 96 steps. Some results are copied from iTransformer table-10 [4], however, the reported results for iTransformer results were reevaluated.

Dataset	SR with SWIN (ours)		Informer		FEDformer		iTransformer		DLinear		FITS	
	MSE	MAE	MSE	MAE	MSE	MAE	MSE	MAE	MSE	MAE	MSE	MAE
ETTm2	0.275	0.39	0.407	0.492	0.203	0.287	0.186	0.272	0.193	0.292	**0.160**	**0.249**
Solar	**0.187**	0.246	0.1931	**0.222**	0.242	0.342	0.206	0.237	0.290	0.378	0.313	0.327
Traffic	0.538	0.896	0.509	0.598	0.587	0.366	**0.403**	**0.276**	0.650	0.396	0.657	0.377
Exchange	0.143	0.289	0.892	0.778	0.148	0.278	0.086	0.206	0.088	0.218	**0.0818**	**0.198**
SCell - Prediction	**0.264**	**0.395**	0.497	0.566	0.504	0.569	0.495	0.564	0.517	0.573	0.510	0.568

Next, to train the random forest training dataset, we extract the features for each data point. We use the validation points as labeled data points, with labels $\{0, 1\}$, where a point is set to belong to class 1 if the SCell prediction performance is satisfactory. Note that since the performance of the AI solution can be evaluated on the validation data points, these labels can be extracted. In this work, we use a threshold on the correlation metric to distinguish between the two classes. An example of the threshold value is 0.9. We then train the Random forest classifier based on the features to identify the feasibility of SCell prediction based on the validation dataset. Our result shows that such a classifier can achieve $\sim 85\%$ accuracy and high impact on Tput see Fig. 6. We plot the solutions for the selected UEs in 6. While all the curves are impacted, we notice that the proposed AI solution demonstrated better predictive ability for the selected UEs, thus achieving more stable performance along the entire band.

B Super-Resolution for Series Forecasting- Sample Results

In this section, we highlight that the proposed solution can also be applied to time-series forecasting. While further enhancements to the design, such as incorporating normalization techniques commonly used in prior work, could yield additional gains, our current results demonstrate competitive performance. As shown in Table 2, the SR-based solution performs on par with state-of-the-art methods across several standard benchmark datasets. For the Scell prediction task (the focus of this workshop paper), we used a smaller subset of the data described in Section 5, consisting of 80 UEs in total.

The methods compared in Table 2 represent state-of-the-art approaches in time-series forecasting, selected for the following reasons. Informer: A well-engineered transformer architecture commonly used as a baseline. FEDformer: Processes time series in the frequency domain, offering an alternative perspective. iTransformer: Challenges conventional time-series representations by rethinking input structure. DLinear: A simple yet effective alternative to transformer-based models, demonstrating strong performance across various tasks. FITS: A lightweight solution that leverages frequency-domain interpolation for forecasting. Like our approach, both FITS and FEDformer incorporate frequency-domain processing. The other architectures focus on variations in complexity and attention mechanisms.